Virology 527 (2019) 64–76

Contents lists available at ScienceDirect

Virology

journal homepage: www.elsevier.com/locate/virology

Glycoprotein D of HSV-1 is dependent on tegument protein UL16 for packaging and contains a motif that is differentially required for syncytia formation

Jillian C. Carmichael[a], Jason Starkey[a], Dan Zhang[a], Akua Sarfo[a], Pooja Chadha[a], John W. Wills[a], Jun Han[a,b,*]

[a] Department of Microbiology and Immunology, The Pennsylvania State University College of Medicine, Hershey, PA 17033, USA
[b] Department of Preventive Veterinary Medicine, China Agricultural University College of Veterinary Medicine, Beijing 100193, China

ARTICLE INFO

Keywords:
Glycoprotein D
Herpes simplex virus
Cell-to-cell spread
Packaging
UL16
Cell fusion, syncytia
Protein interactions
Tegument

ABSTRACT

Glycoprotein D (gD) of herpes simplex virus type 1 (HSV-1) plays a key role in multiple events during infection including virus entry, cell-to-cell spread, and virus-induced syncytia formation. Here, we provide evidence that an arginine/lysine cluster located at the transmembrane-cytoplasm interface of gD critically contributes to viral spread and cell-cell fusion. Our studies began with the discovery that packaging of gD into virions is almost completely blocked in the absence of tegument protein UL16. We subsequently identified a novel, direct, and regulated interaction between UL16 and gD, but this was not important for syncytia formation. However, a mutational analysis of the membrane-proximal basic residues of gD revealed that they are needed for the gBsyn phenotype, salubrinal-induced fusion of HSV-infected cells, and cell-to-cell spread. Finally, we found that these same gD tail basic residues are not required for cell fusion induced by a gKsyn variant.

1. Introduction

An estimated 67% of adult humans are latently infected with herpes simplex virus type 1 (HSV-1) (Looker et al., 2015). Dissemination of the virus occurs through two distinct mechanisms. With cell-free spread, newly made virions are released from an infected cell and subsequently enter uninfected cells to repeat the cycle. This perpetuates infection within the host and can also facilitate virus spread to a new host. Additionally, HSV-1 utilizes a cell-to-cell spreading mechanism, in which virions are transported to lateral junctions and pass directly into adjacent, uninfected cells (Johnson and Huber, 2002; Mateo et al., 2015). This poorly understood mechanism, rather than cell-free spread (Sattentau, 2008), allows the virus to move from the initial site of infection in epithelial cells into sensory neurons, where latency is established (Smith, 2012). When reactivation occurs, cell-to-cell spread enables passage of virions directly from axonal termini into adjacent epithelial cells, enabling HSV-1 to evade neutralizing antibodies from the host response (Kramer and Enquist, 2013; Smith, 2012).

Although they are distinct mechanisms, cell-free and cell-to-cell spread require some of the same proteins. The cell-free entry process begins when glycoprotein D (gD) binds to one of its host receptors, nectin-1, HVEM, or 3-O-HS (Geraghty et al., 1998; Krummenacher et al., 1998; Shukla et al., 1999; Whitbeck et al., 1997). This binding event alters the conformation of gD, which transmits a signal through heterodimer gH/gL to the viral fusogen, gB (Atanasiu et al., 2010; Subramanian and Geraghty, 2007). Once triggered, gB facilitates fusion of the viral envelope with the host cell, either at the plasma membrane or within an endocytic vesicle (Cooper and Heldwein, 2015). Detailed analyses of how these four glycoproteins (termed the "fusion machinery") facilitate fusion have been possible with a transfection assay in which co-expression of gD, gH/gL, and gB stimulates extensive cell fusion to produce multinucleated cells, which are also known as syncytia (Turner et al., 1998). While the fusion machinery by itself is highly fusogenic, cells infected with the wild-type virus do not exhibit syncytia, indicating that other viral proteins keep the machinery under tight control.

Cell-to-cell spread also requires the fusion machinery (Cheshenko and Herold, 2002) and is tightly regulated to prevent syncytia formation while the viral fusion machinery accumulates at cell junctions. However, alterations to any one of four specific viral proteins or at least one host protein can dysregulate the fusion machinery. In the case of viral Syn mutants, which frequently arise in cell culture (Ambrosini and Enquist, 2015; Wheeler, 1960), the majority map to the cytoplasmic tail of gB (Bond and Person, 1984; Gage et al., 1993) and to gK, a

* Correspondence to: Department of Preventive Veterinary Medicine, China Agricultural University, Beijing 100193, China.
E-mail address: hanx0158@cau.edu.cn (J. Han).

https://doi.org/10.1016/j.virol.2018.09.018
Received 20 August 2018; Received in revised form 24 September 2018; Accepted 24 September 2018
Available online 19 November 2018
0042-6822/

glycoprotein involved in virion envelopment (Dolter et al., 1994; Hutchinson et al., 1992; Pogue-Geile et al., 1984); however, syncytial alterations also occur in UL20 (Melancon et al., 2004), a membrane protein and binding partner of gK, and in UL24, a cytoplasmic protein (Sanders et al., 1982). Independent of viral mutations, syncytia formation also can be induced with wild-type HSV-1 by treating the infected cells with salubrinal (Bryant et al., 2008). Although the target of this drug is unknown, inhibitors of protein tyrosine phosphatase 1B (PTP1B) block salubrinal-induced cell fusion and cell-to-cell spread, suggesting that the viral machinery is regulated by phosphorylation (Carmichael et al., 2018).

Cell-to-cell spread and syncytia formation both require additional viral proteins. For instance, when glycoprotein E (gE) is absent, virus production is not affected, but cell-to-cell spread is blocked, and the virus is limited to cell-free spread (Neidhardt et al., 1987). In cell cultures, this loss results in small plaques (Balan et al., 1994; Polcicova et al., 2005), and in animal models, there is a failure to establish latency in neurons (Dingwell et al., 1994, 1995; McGraw and Friedman, 2009; Saldanha et al., 2000). Within the context of gBsyn variants, elimination of gE results in a mutant that can no longer cause cell fusion (Chatterjee et al., 1989; Davis-Poynter et al., 1994). This is also the case for gBsyn mutants that lack any one of the three tegument proteins that assemble on the cytoplasmic tail of gE, namely UL11, UL16, and UL21 (Han et al., 2011, 2012; Yeh et al., 2011).

The experiments described here began with studies of an HSV-1 mutant that lacks tegument protein UL16 (Starkey et al., 2014). In subsequent studies of this null mutant, we were surprised to find it was greatly diminished in its ability to package gD. This raised the possibility that UL16 and its binding partners might control the Syn phenotype of gBsyn mutants by binding to the cytoplasmic tail of a glycoprotein other than gE. While our findings argue against that hypothesis, they revealed a patch of membrane-proximal basic residues in the cytoplasmic tail of gD that is not required for virus entry but is critically important for both the gBsyn phenotype and cell-to-cell spread.

2. Results

2.1. Diminished incorporation of gD into virions in the absence of UL16

While analyzing our UL16-null virus (ΔUL16) (Starkey et al., 2014), we unexpectedly found that packaging of gD was greatly reduced, even though its cellular expression level was only modestly affected (Fig. 1). As expected, the previously reported defect in expression and packaging of UL11 (Starkey et al., 2014), a well-known binding partner of UL16 (Loomis et al., 2003), was also observed. Although non-detectable with a conventional western blot, at least a few copies of gD must have been packaged into ΔUL16 virions because this glycoprotein is absolutely required for virus entry (Johnson and Ligas, 1988; Ligas and Johnson, 1988), and mutant ΔUL16 is replication competent (Starkey et al., 2014). Furthermore, the reduction in gD packaging was not due to unexpected alterations elsewhere in the viral genome, because wild-type gD levels were restored by inserting the U_L16 gene back in its normal position (ΔUL16. R) or in the place of the U_L35 gene (ΔUL16.Rev35) (Fig. 1), which encodes a minor capsid protein not required for viral replication in cell culture (Desai et al., 1998). These findings suggested the possibility that gD and UL16 might interact.

2.2. UL16 directly binds to the cytoplasmic tail of gD

To test whether UL16 interacts with the tail of gD, three experiments were done. First, the cytoplasmic tail of gD (gD.CT) was expressed as a GST fusion protein (GST-gD.CT), purified with glutathione beads, and incubated with lysates of cells infected with wild-type HSV-1 or mutants lacking UL11 or UL16. The previously described fusion proteins GST-UL11(1–50) and GST-gE.CT (containing the cytoplasmic tail of gE) were used as positive controls, both of which directly bind to UL16 (Han et al., 2011; Yeh et al., 2008). GST-gD.CT was able to pull down UL16 from virus-infected cells; however, unlike GST-UL11(1–50), this interaction was much more efficient at 37 °C (Fig. 2A). The pull-down was not dependent on UL11, and GST alone did not pull down UL16, even at 37 °C.

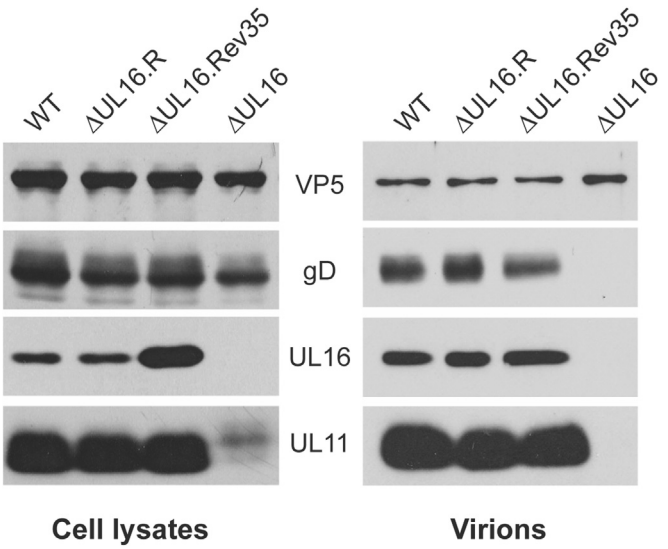

Fig. 1. UL16 is critical for gD packaging. Vero cells were infected with WT, UL16-null mutant, or repaired (ΔUL16.R or ΔUL16.Rev35) viruses at an MOI of 1. At 24 h post infection, extracellular virions in the media were pelleted through a 30% sucrose cushion, and the collected cells were lysed with SDS-PAGE loading buffer. Samples were analyzed by western blotting with antibodies specific for the indicated viral proteins.

In the second experiment, we tested whether the gD-UL16 interaction requires the presence of other viral proteins. For this, Vero cells were transfected with plasmids encoding UL16-GFP or free GFP. At 24 h post transfection, cell lysates were prepared and incubated with GST-gD.CT beads. Again, UL16-GFP, but not GFP, was readily pulled down at 37 °C (Fig. 2B), but not at RT (data not shown), suggesting that the interaction is independent of other viral factors, as is the case for binding of UL16 to UL11 and gE (Fig. 2B) (Yeh et al., 2011, 2008).

In the third experiment, we tested whether the gD-UL16 interaction requires any eukaryotic factors by producing these proteins in bacteria for an *in vitro* binding assay. A His_6-tagged UL16 was purified as described previously (Yeh et al., 2008), and increasing amounts were incubated with GST-gD.CT beads for 2 h at 37 °C. The GST protein served as a negative control. As expected, GST alone did not bind to UL16 (Fig. 2C). In contrast, GST-gD.CT was able to pull down His_6-UL16 in a dose-dependent manner (Fig. 2C). These data demonstrate that UL16 can bind directly with the tail of gD without assistance from any eukaryotic host factors.

2.3. Regulated interaction between UL16 and gD

We next asked whether UL16 and gD associate when they are co-expressed in Vero cells. To visualize the subcellular location of gD, an HA epitope tag was fused to its C-terminus, and this construct was co-expressed with UL16-GFP (Fig. 3A). In contrast to the efficient interactions seen with the *in vitro* assays, there was only partial colocalization between the two proteins in this assay with most of the UL16-GFP remaining in the nucleus (Fig. 3A, row 2). This was not surprising because we have previously shown that the C-terminal domain (CTD) of UL16 (residues 156–373) negatively regulates the ability of the N-terminal domain (NTD; residues 1–155) to bind to gE, UL11, and VP22 (Chadha et al., 2012; Starkey et al., 2014; Yeh et al., 2011). To test whether this is also true for the gD-UL16 interaction, gD.HA was

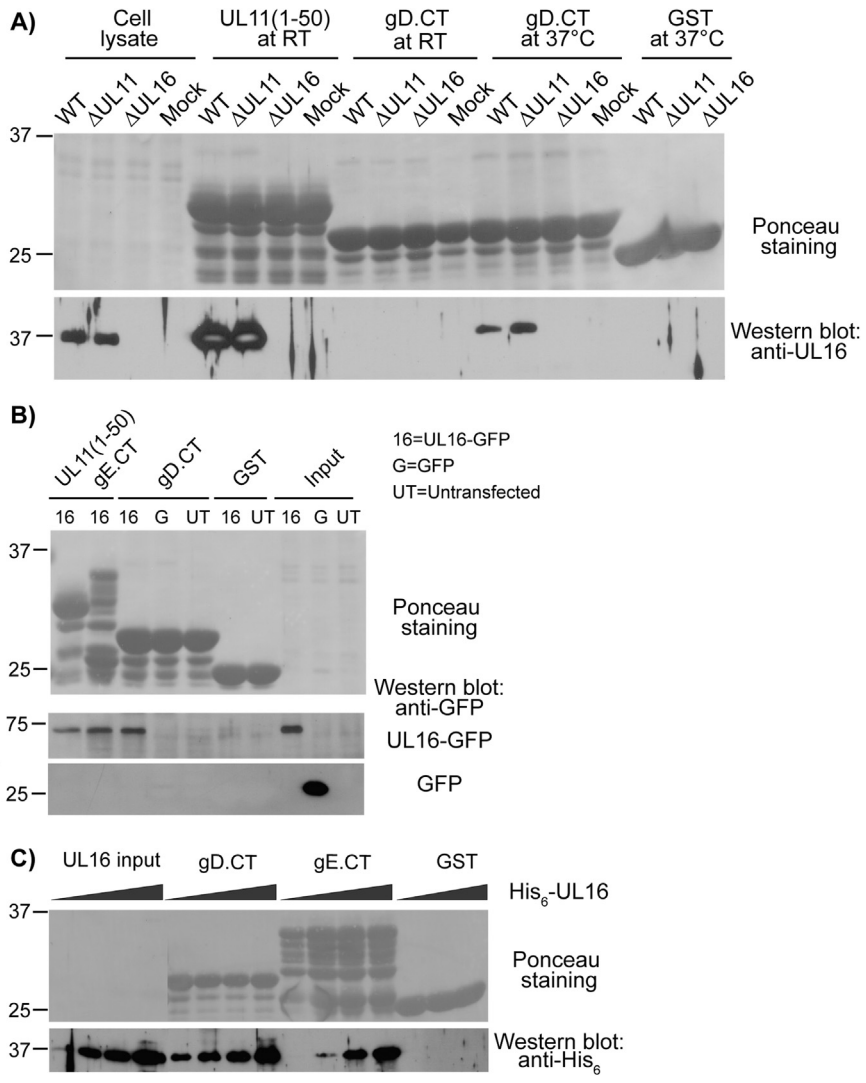

Fig. 2. UL16 interacts with the cytoplasmic tail of gD. (A) Vero cells were infected with WT, ΔUL11, or ΔUL16 viruses. At 24 h post infection, cell lysates were prepared and incubated with the purified fusion proteins GST-UL11(1–50), GST-gD.CT, or GST-only, as indicated on the top panel, and a Ponceau stain for total protein was performed. After 5 h of incubation at room temperature or at 37 °C, the beads were washed, boiled in sample buffer, and the proteins were analyzed by western blotting with an antibody specific for UL16. (B) Vero cells were transfected with expression plasmids for UL16-GFP or GFP-only. At 18–24 h post transfection, cell lysates were prepared and incubated with the purified fusion proteins GST-UL11(1–50), GST-gE.CT, GST-gD.CT, or GST-only, as indicated on the top panel, and a Ponceau stain for total protein was performed. After incubation, the beads were processed as in (A) and an antibody specific for GFP was used. (C) Increasing amounts of purified His_6-UL16 produced in *E. coli* was incubated with GST-gD.CT, GST-gE.CT, or GST-only bound to glutathione-sepharose beads in 0.5% NP-40 buffer at 37 °C. After incubation, the beads were processed as in (A), a Ponceau stain for total protein was performed, and an antibody specific for the His tag was used to probe the western blot.

coexpressed with UL16 NTD-GFP or UL16 CTD-GFP, which by themselves are strongly localized to the nucleus (Fig. 3A, top row). When coexpressed with gD.HA, the CTD did not respond (row 3); however, the NTD was dramatically and completely relocalized to the cytoplasm (row 4).

The NTD interaction was also observed when GST-gD.CT was used in a pull-down assay with purified His_6-UL16(1–155) at 37 °C, and the efficiency was similar to that for GST-gE.CT and GST-UL11 (Fig. 3B). Moreover, treatment of His_6-UL16(1–155) with N-ethylmaleimide (NEM), a small chemical that covalently modifies free cysteines, did not affect the pull-down, unlike the interaction of UL16 with UL11 (Yeh et al., 2008). This suggests that the five cysteines in the UL16 NTD are not involved, and the site in UL16 that binds to gD is distinct from that used for UL11 binding.

2.4. The UL16-gD interaction is not critical for the gBsyn phenotype

Since UL16 is known to be required for gBsyn-mediated cell fusion (Han et al., 2012), we asked whether its binding to gD is also important for this phenotype. If it is, then gD-tail mutants that are unable to bind UL16 should be non-fusogenic, even in the presence of a gBsyn mutation. To test this, gD-tail truncations were built into a virus containing the gB.A855V *syn* mutation. The first mutant, ΔCT (Fig. 4), lacks the entire cytoplasmic tail (residues H_{365}-Y_{394}) as the result of a stop codon inserted in place of M_{364}. While the parental gBsyn virus produced extensive, large syncytia in infected Vero cells, the ΔCT/syn virus produced only small, lytic plaques (Fig. 5A). The mutant virions still packaged and retained the truncated form of gD, even though there were no charged residues adjacent to the transmembrane sequence (Fig. 5B, right panel), and the gBsyn phenotype was restored when the tail was repaired (Fig. 5A, ΔCT.R/syn). Thus, it seemed possible that UL16 binding might be required for cell fusion.

To delineate the region required for the gBsyn phenotype, additional gD-tail truncations were examined. Mutant M5/syn has a stop codon in place of residue P_{372} (Fig. 4) and remained syncytial (data not shown), as did the even shorter M6/syn mutant (Fig. 5A), which retains only the membrane-proximal HRR residues (Fig. 4). Moreover, the amount of gD packaged into M6/syn virions was about the same as for mutant ΔCT/syn, which is not syncytial (Fig. 5B, right panel), suggesting that the additional MHRR sequence is simply needed for cell fusion. However, compared to the gBsyn parent and mutant M6/syn, ΔCT/syn was greatly impaired in its ability to replicate and spread when Vero cells were infected at a low MOI (Fig. 5C).

To assay for UL16 binding, the tails of M5 (MHRRTRKA) and M6 (MHRR) were fused to GST and purified for pull-down assays. Binding of His_6-UL16 was greatly diminished for the M5 construct and undetectable with the M6 construct (Fig. 5D). Since the gBsyn viruses expressing these shortened gD tails remain syncytial, it appears that the gD-UL16 interaction is not required, in contrast to what was found for gBsyn mutants lacking the tail of gE (Han et al., 2012). However, it

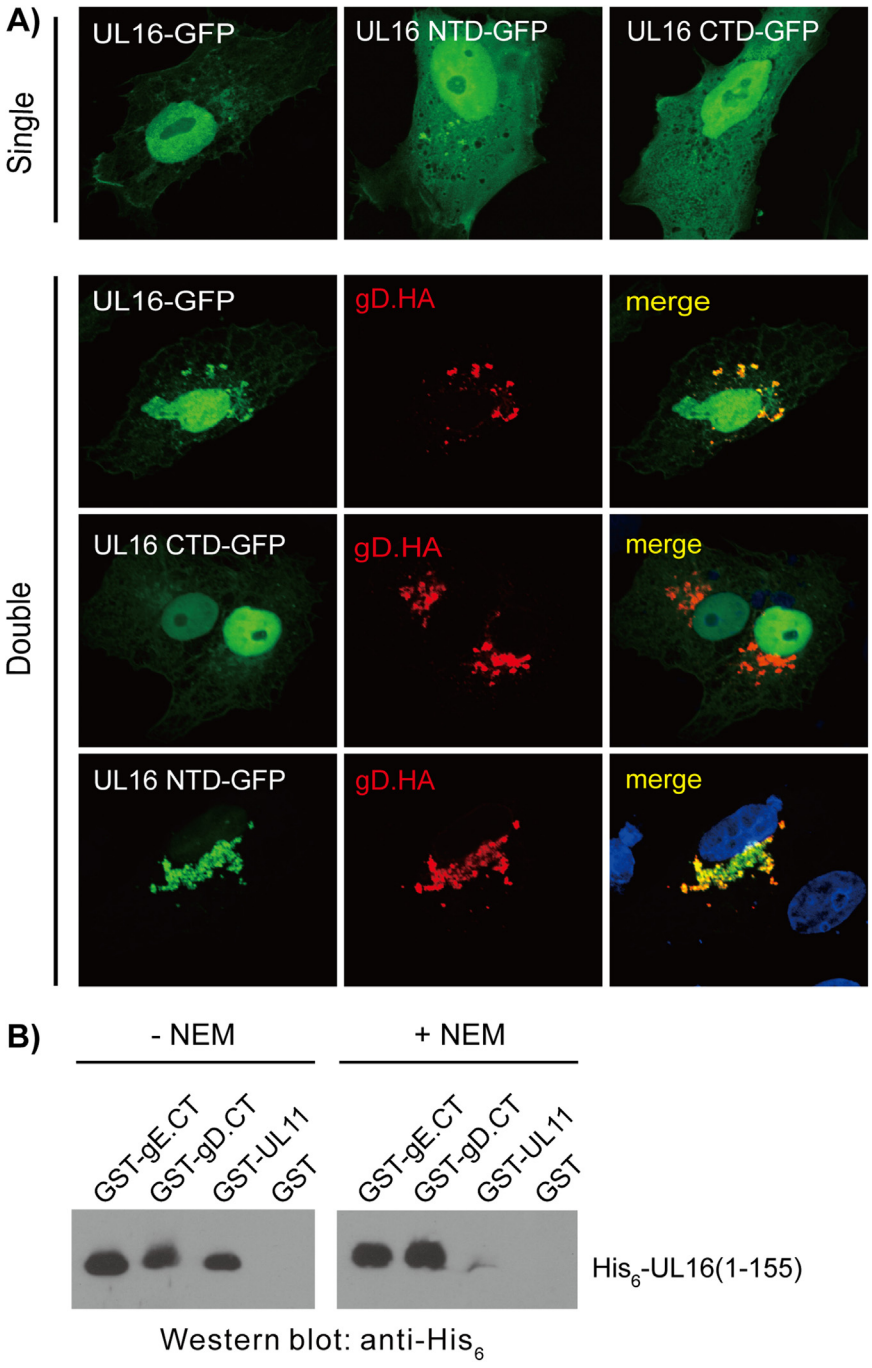

Fig. 3. A regulated interaction between UL16 and the gD cytoplasmic tail. (A) Vero cells were singly transfected (top row) with plasmids that express full-length UL16-GFP, UL16 NTD-GFP, or UL16 CTD-GFP. Additionally, each of these constructs were co-expressed with gD-HA (bottom three rows). Cells were fixed, permeabilized, and stained with a monoclonal antibody against the HA tag at one day post-transfection. (B) Purified His_6-UL16(1–155) protein was incubated with the indicated GST-fusion proteins either in the presence or absence of NEM bound to glutathione-sepharose beads in 0.5% NP-40 buffer at 37 °C. The beads were then washed, boiled in sample buffer, and the proteins were analyzed by western blotting.

remains possible that the gD-UL16 interaction is needed for some other event (e.g., perhaps *in vivo*).

Because gD packaging was undetectable by conventional western blotting in the absence of UL16 (Fig. 1), we wondered whether the reverse was true. Analyses of mutants ΔCT/syn and M6/syn showed normal amounts of UL16 in the extracellular virions (Fig. 5B, right panel), although in this particular experiment, a loading error for the wild type can be seen by the presence of a reduced amount of VP5, the major capsid protein. Nevertheless, it is clear that packaging of UL16 does not require its interaction with gD, and previous studies have revealed other binding partners upon which UL16 is highly dependent (Meckes et al., 2010). Other examples of nonreciprocal packaging have been found among interacting tegument proteins and glycoproteins. For example, gE packaging is greatly reduced when binding partner VP22 is absent, but when the tail of gE is absent, this tegument protein is still packaged to normal levels (O'Regan et al., 2010; Starkey et al., 2014).

2.5. Importance of basic residues in the gD tail for the gBsyn phenotype

Based on the properties of mutants ΔCT/syn and M6/syn, we hypothesized that the MHRR sequence is important for the gBsyn phenotype and virus spreading. To further test this, we constructed additional cytoplasmic tail mutants in the gBsyn background and measured their plaque sizes and fusogenic activity. Deletion of the HRR residues from M6/syn (mutant M7/syn, Fig. 4) reduced plaque size by 90% (Fig. 6A) and caused a loss of the gBsyn phenotype (Fig. 6B), as was seen for the ΔCT/syn mutant. Reinsertion of the complete tail sequence (M7.R/syn) resulted in normal sized plaques (Fig. 6A) and syncytia formation (not shown). Mutants M5/syn and M6/syn also had reduced plaque sizes, but the defects were not as severe as for M7/syn (Fig. 6A).

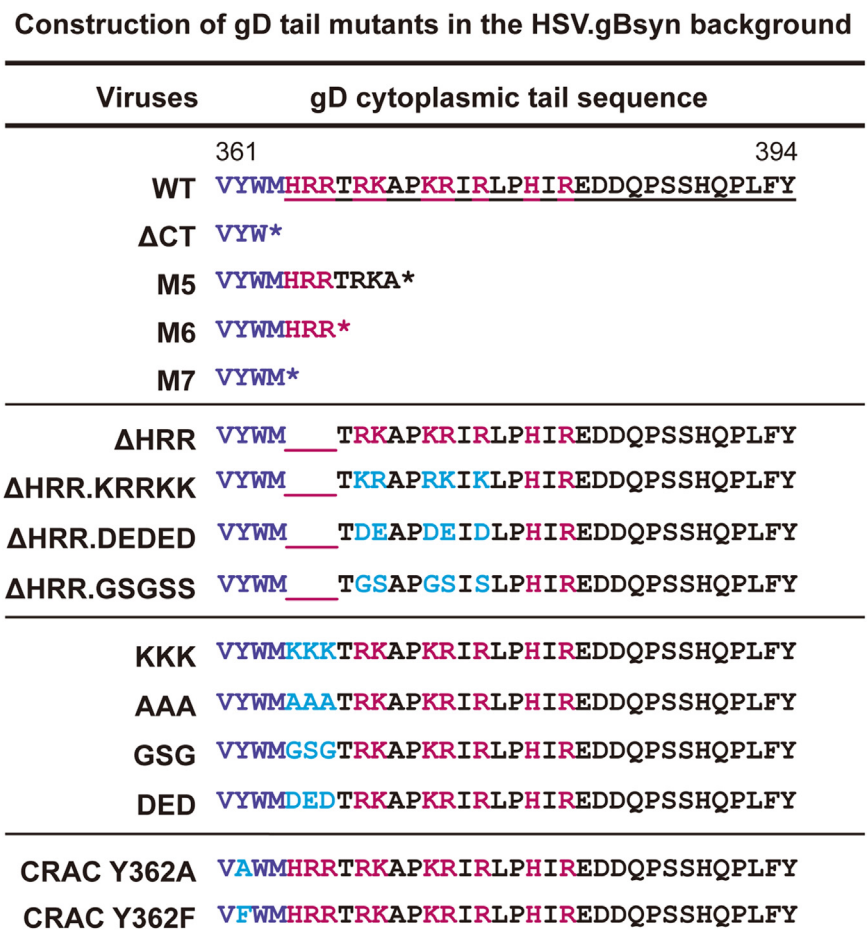

Fig. 4. Mutants of the gD tail used in this study. The wild-type sequence of the gD tail is underlined with basic residues indicated with pink text and the transmembrane residues indicated by purple text. The mutants are grouped into four categories based on the type of changes made. Mutants in which stop codons have been inserted are marked with asterisks. Mutants with deleted residues are marked with an underscore where the residues used to be. Mutants where residues have been altered are indicated with blue text.

If the HRR sequence is critical, then its removal from an otherwise full-length gD might be expected to eliminate the gBsyn phenotype, and to test this, we constructed mutant ΔHRR/syn and a repaired virus ΔHRR.R/syn (Fig. 4). The HRR deletion had no effect on plaque size (Fig. 6C) or virus-mediated cell fusion (Fig. 6B). However, a closer examination of the tail sequence revealed seven additional, downstream basic residues (Fig. 4; R369, K370, K373, R374, R376, H380, and R381). Since the ΔHRR/syn virus is fully fusion competent, we considered the possibility that these downstream basic residues can be moved up to compensate for the missing HRR residues. To test this, three mutants were constructed that altered the five closest basic residues: a same-charge mutant (ΔHRR.KRRKK/syn), an opposite-charge mutant (ΔHRR.DEDED/syn), and a mutant with uncharged residues (ΔHRR.GSGSS/syn) (Fig. 4). As anticipated, the same-charge substitution mutant (KRRKK) remained fully fusogenic, but substitutions DEDED and GSGSS completely blocked syncytia formation (Fig. 6B). These results suggest that having basic residues close to the transmembrane region of gD is critical for the gBsyn phenotype.

We also made substitutions within the HRR motif without altering the length of gD (Fig. 4). As predicted, a mutant with a same-charge substitution, KKK/syn, was like the gBsyn parent with regard to syncytia formation (Fig. 6B) and plaque size (Fig. 6C), but a reversal-of-charge mutant, DED/syn, was unable to fuse cells (Fig. 6B) and produced tiny plaques (Fig. 6C), similar to deletion mutants M7/syn and ΔCT/syn. These properties were not due to unintended mutations in other genes as a repaired virus (DED.R/syn) behaved like the gBsyn parent (Fig. 6C). In contrast, two mutants with uncharged amino acids in place of HRR, AAA/syn and GSG/syn, produced plaques of intermediate size (Fig. 6C) and were still able to fuse cells, albeit at reduced levels (Fig. 6B). Thus, it appears that nearby basic residues can serve in the place of HRR to some degree unless membrane-proximal negative charges are present.

In the course of these studies, we noticed that the sequence upstream of HRR contains a potential cholesterol recognition consensus (CRAC) motif: (L/V)-X1–5-(Y)-X1–5-(K/R) (Fantini et al., 2016). These are typically located at transmembrane-cytoplasm interfaces, and in gD, the sequence is LVICGIVYWMHRR. Evidence against this motif being important was provided by mutants AAA/syn and GSG/syn, which were syncytial even though the spacing between Y362 and the downstream basic residue had been altered to be one residue longer than specified by the CRAC motif (Fig. 6B). Nevertheless, we constructed two additional mutants in the gBsyn virus in which the invariant tyrosine (Y362) was changed to alanine or phenylalanine (Fig. 4). Both mutants were able to induce cell-cell fusion (Fig. 6D), clearly demonstrating that the CRAC motif is not required for the gBsyn phenotype.

2.6. Importance of membrane-proximal basic residues for virus replication and spread

Because mutants M7/syn and DED/syn produced very small plaques like those of mutant ΔCT/syn, the yields of infectious virions for these three mutants were compared relative to the gBsyn parent. For this, cells were infected at a low MOI (0.1), and the infection was allowed to spread for 30 h, after which the titers of cell-associated and extracellular viruses were measured (Table 1). Although the total yields for M7/syn and DED/syn were not reduced as severely as for mutant ΔCT/syn, they were still nearly a log lower than those of the parent virus. However, all three gD mutants were similar in that a greater percentage of the total infectivity was cell-associated compared to the parent. This suggests that the mutants have a virion egress defect, which would reduce the ability of the infection to spread through the culture as fast as the parent and result in lower virus yields. To test this hypothesis, the

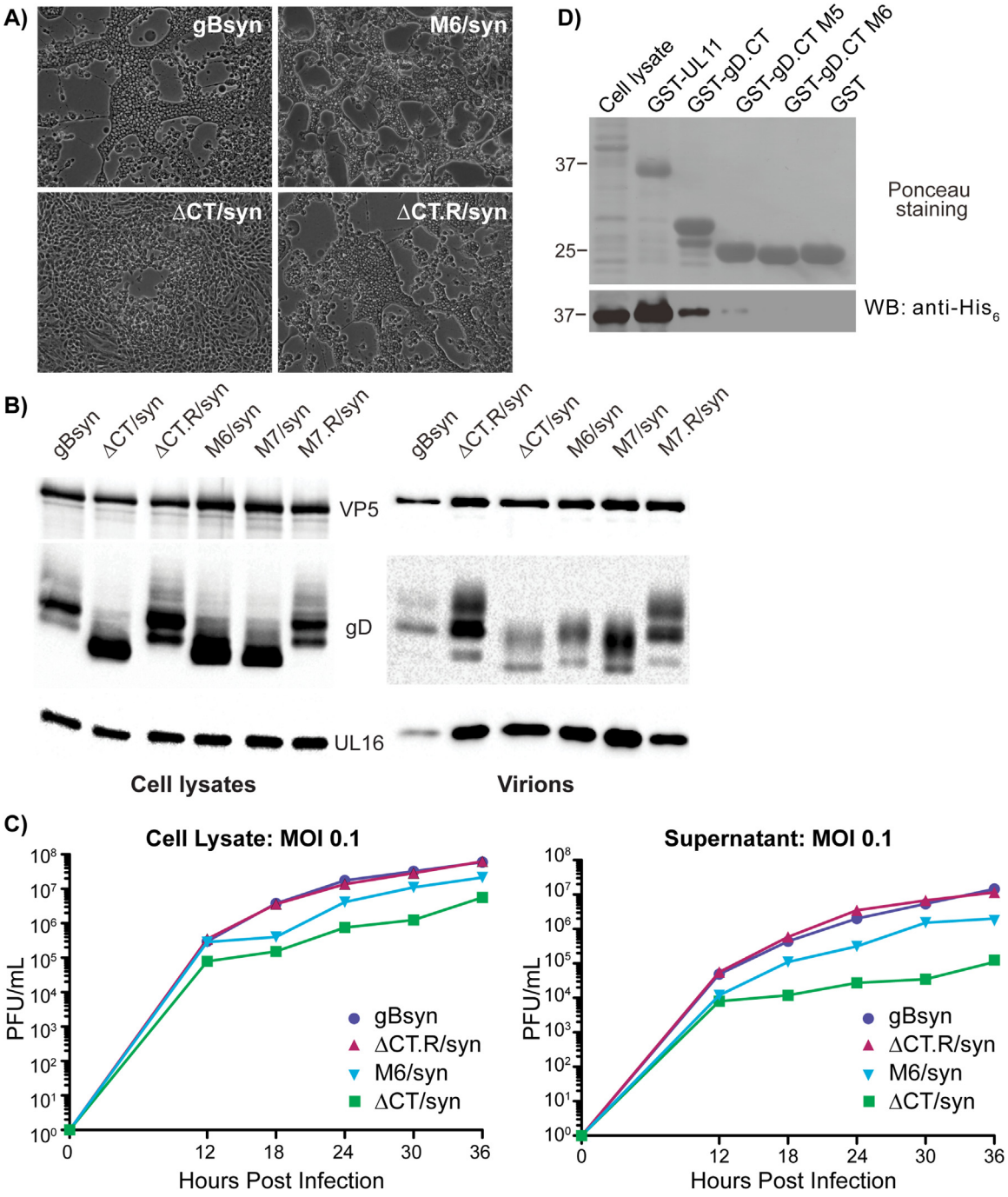

Fig. 5. The UL16-gD interaction is not critical for the gBsyn phenotype. (A) Cells were infected with gBsyn, M6/syn, ΔCT/syn, or ΔCT.R/syn at a low MOI. Images were taken with an inverted light microscope at 2–3 days post infection. (B) Vero cells were infected with the indicated viruses at an MOI of 1. At 24 h post infection, extracellular virions in the media were pelleted through a 30% sucrose cushion and the cells were collected. Samples were analyzed by western blotting. (C) Duplicate cultures of Vero cells were infected with the indicated viruses at an MOI of 0.1. The media containing extracellular virions was collected, and the infected cells were harvested and processed separately at 6-h time points. Infectious virus was titered by plaque assay. (**D**) Purified His_6-UL16 was incubated in 0.5% NP-40 buffer at 37 °C for 5 h with glutathione-sepharose beads bearing GST fusion proteins with the entire tail of gD or truncated sections of the tail. GST-UL11 and GST alone served as respective positive and negative controls. After incubation, the beads were washed, boiled in sample buffer, and the presence of bound His_6-UL16 was analyzed by western blotting.

replication of mutants M7/syn and DED/syn were examined in a high MOI experiment so as to remove the compounding effects of virus spreading (Fig. 7A). Both of the mutants were similar to the parent in regard to their levels of cell-associated virus, but infectious virus was slower to be released into the medium and never reached the level of gBsyn (Fig. 7A). Thus, the small-plaque and non-syncytial phenotypes of M7/syn and DED/syn are not due to reduced virion production but more likely result from a defect in cell-to-cell spread.

In the most common *in vitro* assay for measuring cell-to-cell spread, only a few infectious virions are added to a monolayer so that individual plaques can be observed and measured. After the initial infection, strongly neutralizing antibodies are added to the growth medium to prevent cell-free spread. Mutants that are defective for cell-to-cell spread will therefore produce smaller plaques compared to

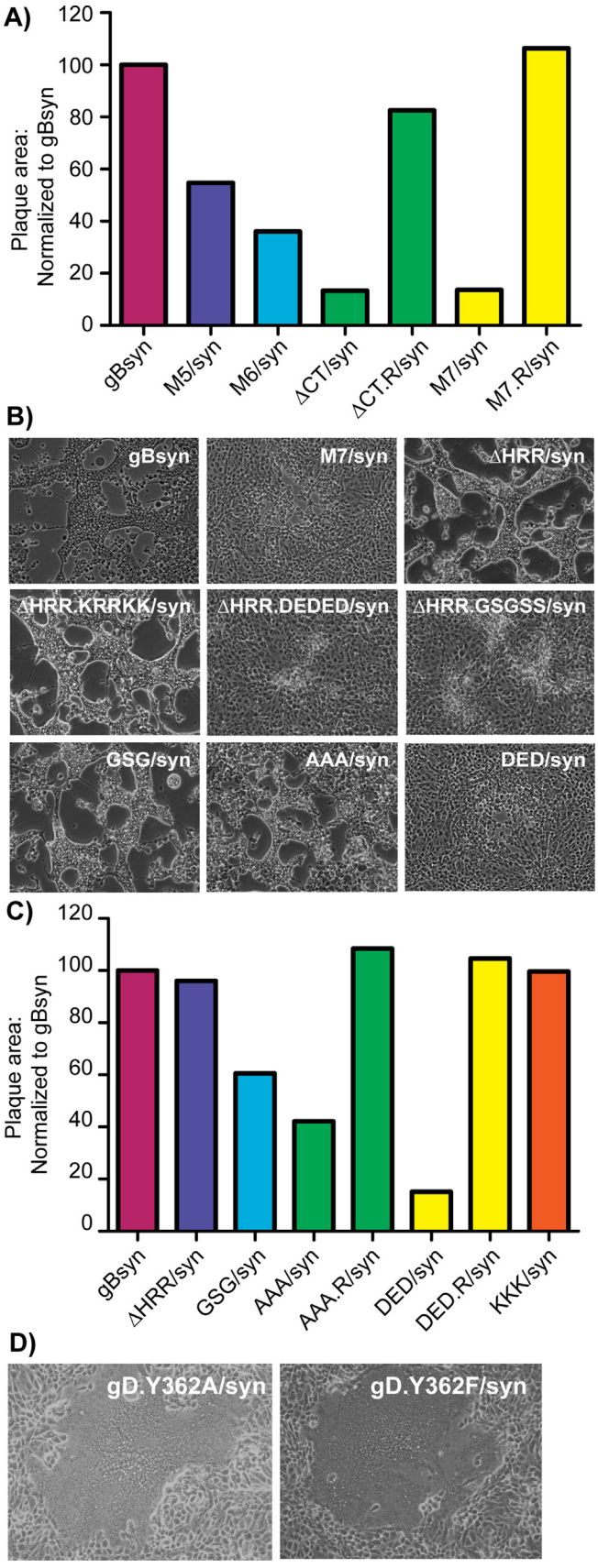

Fig. 6. Membrane-proximal gD basic residues are important for the gBsyn phenotype and plaque size. (A) Vero cells were infected at a low MOI with the indicated gD mutants. After infection, the cells were rinsed, overlaid with methylcellulose, and incubated at 37 °C. At 4 days post infection, the cells were fixed and stained with crystal violet. The plates were imaged, and the areas of 20 representative plaques for each virus were measured using ImageJ. Plaque size is plotted as normalized to gBsyn. (B) Vero cells were infected with the indicated viruses at a low MOI. Images were taken at 2–3 days post infection with an inverted light microscope. (C) Vero cells were infected with the indicated gD mutants and analyzed as described in (A). (D) Vero cells were infected with gD.Y362A/syn or gD.Y362F/syn. Images of individual syncytia were taken 24 h post infection.

Table 1
Viral yields[a] after low MOI[b] infection.

Viral pfu/ml (% of Total)			
Virus	**Intracellular**	**Media**	**Total**
gBsyn	4×10^7 (82%)	8.5×10^6 (18%)	4.85×10^7
ΔCT/syn	2×10^6 (97%)	5.75×10^4 (3%)	2.06×10^6
M7/syn	5.38×10^6 (94%)	3.25×10^5 (6%)	5.7×10^6
DED/syn	5.75×10^6 (94%)	3.25×10^5 (6%)	6.1×10^6

[a] Virus harvested at 30 h post infection.
[b] MOI of 0.1.

spreading competent controls.

Although mutants M7/syn and DED/syn are not syncytial and exhibited dramatic cell-to-cell spreading defects in the presence of neutralizing antibodies (not shown), two new viruses were made, M7 and DED, which have the same changes to gD but lack the *syn* mutation. In a high MOI replication assay, mutants M7 and DED produced slightly less intracellular virus than WT, with a clear delay for the DED virus, and as expected, the amount of extracellular virus was markedly reduced by 1–2 logs (Fig. 7B). When these viruses were used in the cell-to-cell spreading assay, both exhibited severe spreading defects as visualized by immunostaining for VP5 (the major capsid protein) (Fig. 7C). In fact, the plaques formed by M7 and DED were only 15% percent the size of WT plaques (Fig. 7D). These results are consistent with the findings of a previous study (Arii et al., 2016), which showed a 50% reduction in plaque size. However, the results shown here are far more dramatic because the basic residues downstream of HRR cannot contribute to spread.

2.7. Basic residues in gD are differentially required for gBsyn, gKsyn, and salubrinal-induced fusion

Because gD is part of the essential fusion machinery, we hypothesized that its basic residues would be required for gKsyn-induced syncytia, just as they are for gBsyn. However, we were not confident in this prediction because recent studies have shown that the Syn phenotypes of HSV-1 are more complex than previously thought. For example, tegument protein UL21 has been found to be essential for the gBsyn phenotype but dispensable for gKsyn (Sarfo et al., 2017). To test our hypothesis, the M7 and DED mutations were combined with the long studied gKsyn mutation A40V (Debroy et al., 1985). Strikingly, both M7/gKsyn and DED/gKsyn were still able to fuse cells (Fig. 8A), although the syncytia formed by these viruses were 60% smaller than those of gKsyn (Fig. 8B). Thus, it appears that while these basic residues are not required for the gKsyn phenotype, virus spreading is still restricted in the M7/gKsyn and DED/gKsyn mutants.

Robust syncytia formation also occurs when cells infected with wild-type HSV-1 are treated with salubrinal (Boyce et al., 2005; Bryant et al., 2008). Although the target of this drug is not know, the mechanism of cell fusion requires UL16 and the cytoplasmic tail of gE (Carmichael et al., 2018). Because those viral proteins are required for the gBsyn

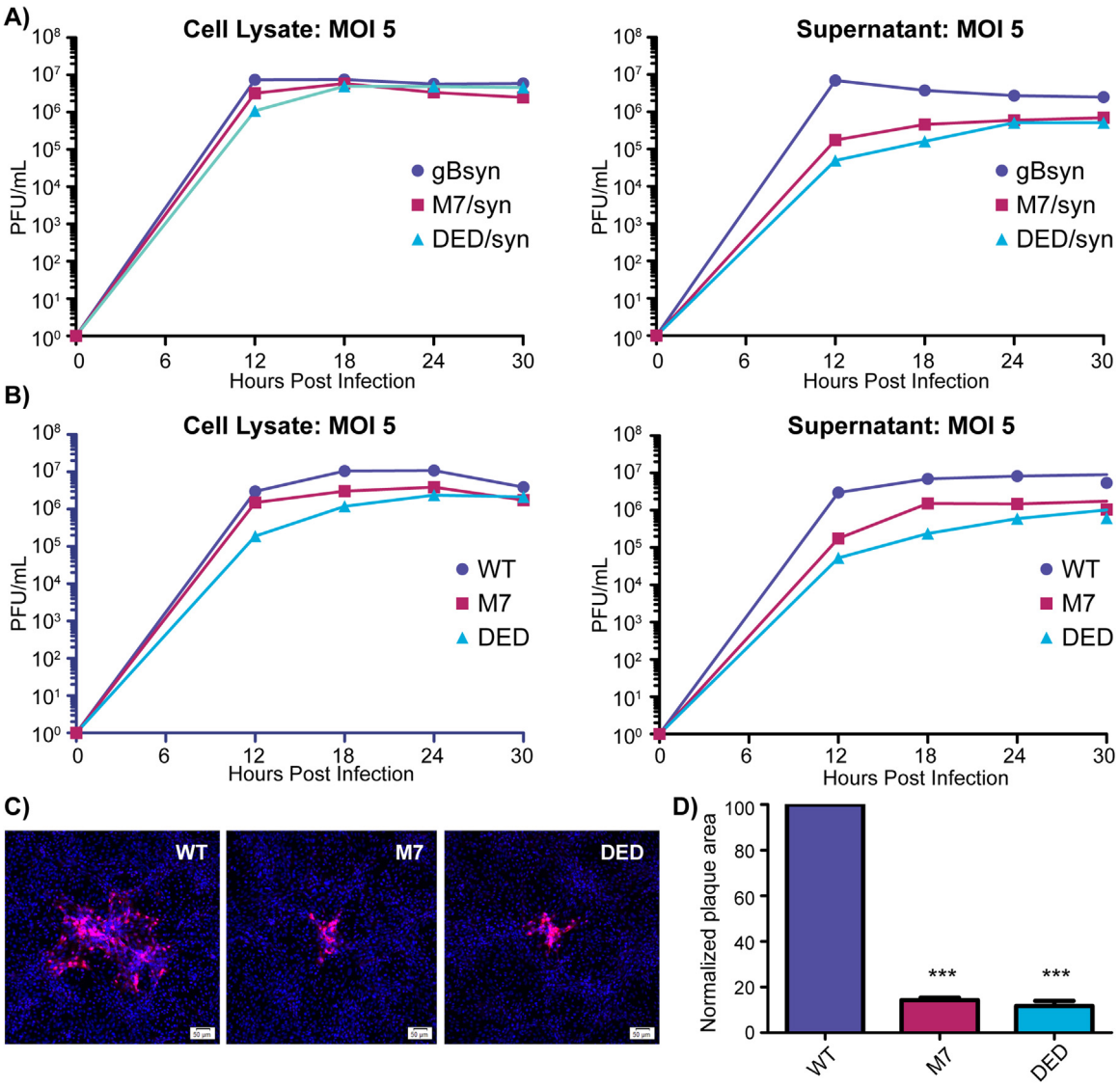

Fig. 7. gD basic residues involvement in viral replication and cell-to-cell spread. (A) Vero cells were infected with gBsyn, M7/syn, or DED/syn viruses at an MOI of 5 for 1 h. After infection, media and cell lysate were harvested separately in 6-h time increments, and samples were analyzed via plaque assay. (B) A single-step growth curve with the same experimental setup as described in (A) was performed for the WT, M7, and DED viruses containing no Syn mutations. (C) Vero cells were infected with WT, M7, or DED a low MOI (0.001) for 1 h. After infection, cells were incubated in DMEM containing 5 mg/ml pooled human IgG. At 48 h post infection, cells were fixed, stained for VP5, and plaques were imaged with a fluorescent microscope. Scale bar is 50 μm. (D) Quantitation of the experiment performed in (C) using Olympus cellSens software. Two independent experiments were performed, 10–15 plaques per sample were measured per experiment, and a Student *T*-test was performed (*** $P < 0.001$).

phenotype, along with the HRR motif of gD, we hypothesized that salubrinal would not stimulate fusion of cells infected with the M7 or DED viruses. To test this, M7 or DED-infected cells were treated with salubrinal and examined 18 h later for syncytia formation via a previously described flow cytometry assay (Carmichael et al., 2018). In contrast to WT-infected cells, essentially no fusion was observed in cells infected with the gD mutants (Fig. 8C).

3. Discussion

Glycoprotein D is a key player for multiple events during HSV-1 infection, including virus entry, capsid envelopment, virus-induced cell fusion, and cell-to-cell spread (Arii et al., 2016; Davis-Poynter et al., 1994; Johnson and Ligas, 1988; Johnson et al., 2011; Lee et al., 2009; Ligas and Johnson, 1988). Most studies of the molecular functions of gD have centered on its extracellular domain, which consists of a large receptor-binding region and a short, proline-rich region that is critical for fusion of the virus envelope with the cell membrane (Fusco et al., 2005; Heldwein and Krummenacher, 2008; Spear et al., 2006). In fact, a soluble form of the gD extracellular domain is sufficient to induce cell fusion when added to cells expressing gB and gH/gL (Atanasiu et al., 2010). This soluble fragment can also rescue the infectivity of a gD-null mutant (Cocchi et al., 2004; Tsvitov et al., 2007), as can a chimera in which the soluble form is attached to the transmembrane domain and cytoplasmic tail from CD8 (Browne et al., 2003). Consistent with this, several studies found that removing most of the gD tail did not drastically lower virus infectivity (Farnsworth et al., 2003; Feenstra et al., 1990; Lee et al., 2009). The experiments described here show that the tail does contain an important function.

3.1. Why is gD packaging reduced in the absence of UL16?

This study began with the observation that tegument protein UL16 is critically important for the packaging of gD. We found that UL16

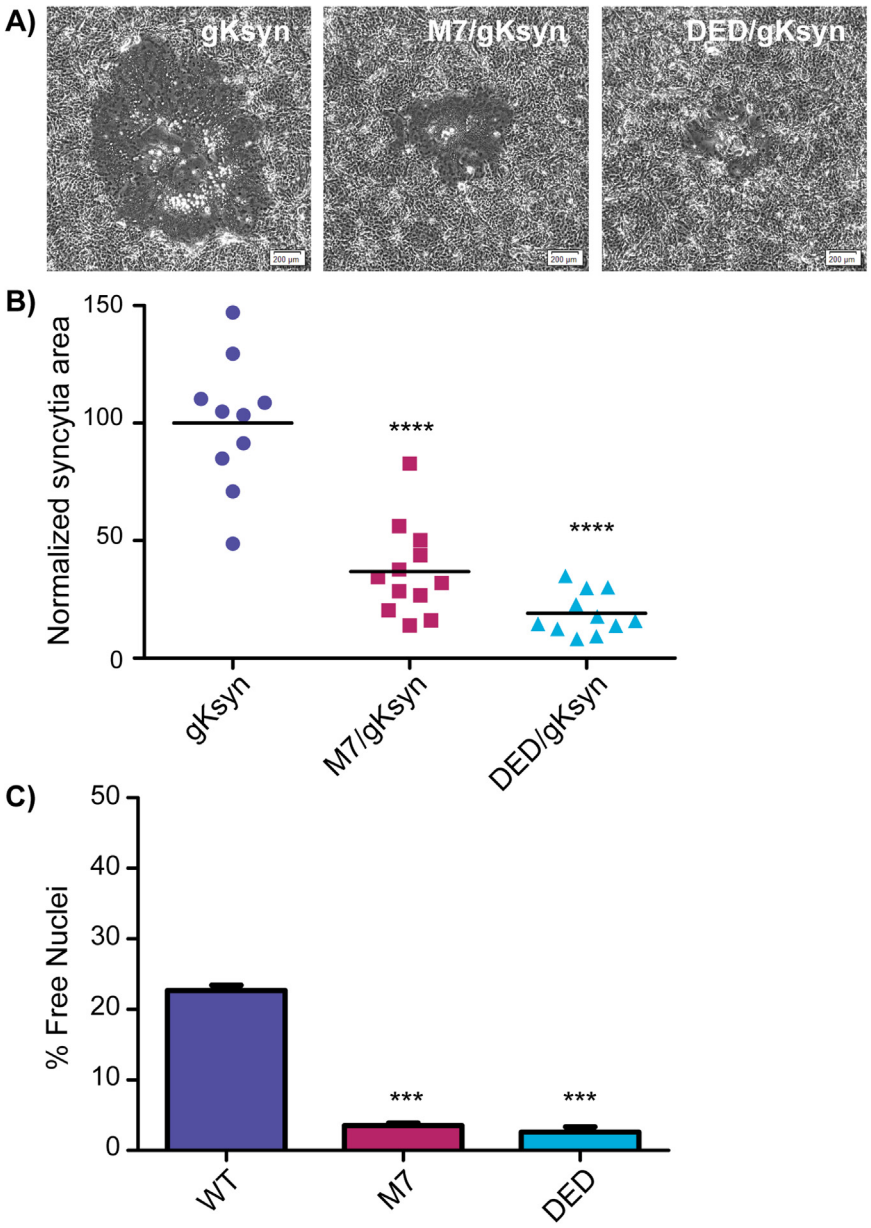

Fig. 8. Differential requirements for basic residues for gKsyn and salubrinal-induced fusion. (A) Vero cells were infected with gKsyn, M7/gKsyn, or DED/gKsyn at a low MOI (0.001) for 1 h and incubated in infection media. At 48 h post infection, individual syncytia were imaged. (B) Quantitative data from the experiment in (A). The areas for 10–12 individual syncytia per virus were measured and plotted around the normalized mean for each virus and a Student T was performed (**** $P < 0.0001$) (C) Vero cells were infected with WT, M7, or DED at an MOI of 3 and were incubated in 50 μM salubrinal. At 18 h post infection, samples were harvested an analyzed via flow cytometry. This experiment was done 3 times and the % free nuclei represents a measure of total cell fusion. Statistical analysis was done by a Student *T* test (*** $P < 0.001$).

binds directly to the cytoplasmic tail of gD at 37 °C, but not at RT, which is reminiscent of the temperature-dependent interaction between VP16 and the cytoplasmic tail of gH (Gross et al., 2003). However, UL16 was still packaged to WT levels when the cytoplasmic tail of gD was removed. This nonreciprocal packaging dependence exhibited is likely a consequence of the complex structure of the tegument. When UL16 is absent, there is a well-documented massive collapse of the protein interaction network in which it resides. For example, it has been shown that gE, UL11, UL21, and VP22 also fail to be packaged in UL16-null virions (Starkey et al., 2014). We hypothesize that the tail of gD is not a critical part of that interaction network and thus, it is not disturbed when the tail is absent. However, the UL16 interaction network appears to be highly important for the proper packaging of gD. Moreover, because UL16 is bound to capsids in extracellular virions (Meckes and Wills, 2007, 2008), it may be that the interaction is important for both the packaging and the positioning of gD within the virion.

The cytoplasmic tail of gD also binds to tegument protein VP22 (Chi et al., 2005). However, the properties of mutant M6/syn demonstrate that this interaction is not important for the gBsyn phenotype or cell-to-cell spread because the binding site for VP22 occurs downstream of the HRR motif (Chi et al., 2005). The same is true for the UL16-gD interaction. Nevertheless, it is possible that the VP22 and UL16 interactions with gD are important during an *in vivo* infection.

Since some of the gD mutants described in this study have replication defects, we were initially concerned that low virus yields might account for the loss of gBsyn-mediated fusion. This is particularly worrisome for Syn mutants that lack UL11 and have replication defects of 100–1000 fold (Fulmer et al., 2007; Han et al., 2011, 2012; Kim et al., 2013; Leege et al., 2009). However, virus replication experiments showed that two of our mutants, M7/gBsyn and DED/gBsyn, clearly do not have severe viral replication defects, and the resulting loss of the gBsyn phenotype is therefore not related to replication. To our knowledge, this is the first evidence of a function within gD that is required for syncytia formation and cell-to-cell spread but not for virus entry. Even more strikingly, another α-herpesvirus, pseudorabies virus, absolutely requires gD for entry, but this glycoprotein is completely dispensable for cell-to-cell spread (Ch'ng et al., 2007; Hanssens et al., 1995).

3.2. What is the role of the membrane-proximal basic residues of gD?

Our experiments have ruled out two potential roles for the basic residues in the tail of gD. First, the virion packaging data for mutants M7 and ΔCT show that no part of the tail is needed for retention of gD in the viral envelope. Indeed, mutant M7 replicates similar to wild-type virus except for its inability to spread cell-to-cell. Second, our studies show that the putative cholesterol-binding motif that overlaps HRR is not essential for the gBsyn phenotype and cell-to-cell spread. However, our results do not rule out a role for cholesterol because five other viral membrane proteins—gM, gK, UL20, UL43, and UL56—contain cholesterol binding motifs at their transmembrane-cytoplasm interfaces. Thus, it is possible that those proteins can bind cholesterol to compensate for loss of the gD motif. The potential role of cholesterol-protein binding in HSV-1 infections warrants further investigation.

Another possibility is that the basic residues enable proper localization of gD within regions containing negatively-charged phospholipids. If this were true, then gD would be mislocalized in the absence of these residues and therefore unable to work in conjunction with other viral proteins such as gE or gM, which are known to function at the cell surface or cellular junctions (El Kasmi and Lippé, 2015; Wisner and Johnson, 2004). Even if gD mutants are at the plasma membrane, they could be localized to the wrong microdomain. This remains to be explored.

Basic residues could also influence the conformation of the extracellular domain of gD in a manner that is critical for cell-to-cell spread and the gBsyn phenotype, but not for receptor binding and virus infectivity. In support of this, replacing the gD tail with that of the PRV homolog reduced binding of polyclonal antiserum R7 to the gD ectodomain by 35% (Zago et al., 2004). Within the first 12 residues of these two cytoplasmic tails, there are eight basic residues in HSV-1 (HRRTRKAPKRIR) but PRV only has three (RGAKGYRLLGGP). It would be interesting to determine if the PRV tail would support the gBsyn phenotype and whether insertion of additional basic residues into the PRV tail would restore binding of R7 antibodies.

Finally, the membrane-proximal basic residues of gD could be involved in membrane deformation. In support of this, during the course of our study, it was reported that wild-type gD will induce the formation of microvillus-like projections from the plasma membrane of transfected cells (Arii et al., 2016). A mutant in which the cluster of membrane-proximal basic residues was replaced with alanines was limited in its ability to induce these projections. Furthermore, when examined in a viral infection, this gD mutant exhibited a 50% reduction in plaque size in the presence of neutralizing antibodies (Arii et al., 2016), indicating a moderate cell-to-cell spread defect. Since our gD mutants either eliminated the tail (M7) or replaced the basic residues with oppositely-charged residues (DED), it is not surprising that we see a considerably stronger cell-to-cell spread defect.

3.3. Differing requirements for the cytoplasmic tail of gD for the induction of syncytia

Syncytia formation can be induced by multiple ways in HSV-1 infected cells. The most well known mechanisms involve mutants that are altered within one of the four *syn* loci, which correspond to the genes for gB, gK, UL20, and UL24. Studies of Syn variants have provided clues to the machinery that regulates the fusion machinery during infection. For instance, studies of Syn variants have identified viral proteins gE/gI, gM/gN, UL45, UL11, UL16, UL21 as being fusion regulators (Davis-Poynter et al., 1994; El Kasmi and Lippé, 2015; Haanes et al., 1994; Han et al., 2012; Kim et al., 2013). However, the mechanisms became more complicated when it was discovered that gBsyn variants require tegument protein UL21 for fusion, but gKsyn, UL20syn, and UL24syn variants do not (Sarfo et al., 2017). Adding to this complexity, the experiments described here show that the membrane-proximal basic residues of gD are needed for the gBsyn phenotype but not that of gKsyn.

Cells infected with HSV-1 can also be induced to fuse by the addition of the small molecule drug named salubrinal (Bryant et al., 2008). The experiments described here demonstrate that the membrane-proximal residues of gD are critical for the mechanism of salubrinal-induced fusion. Salubrinal has complex effects on cells infected with Syn variants, with gBsyn-infected cells being further stimulated to fuse while gKsyn-infected cells cannot fuse in response to this drug (Carmichael et al., 2018). These results clearly indicate that the molecular mechanism driving the gKsyn phenotype differs from that of gBsyn. Whether the fusion complex formed in gBsyn variants is different from that in gKsyn variants, or the same fusion complex is temporally regulated at different steps remains to be seen. Overall, this study reveals a new role for the membrane proximal basic residues in the tail of gD for regulating the fusion machinery during cell-to-cell spread and syncytia formation.

4. Materials and methods

4.1. Cells, virus strains, and antibodies

Vero cells were maintained in Dulbecco's modified Eagle's medium (DMEM; Gibco) supplemented with 5% fetal bovine serum (FBS) and 5% fetal calf serum (FCS), penicillin, and streptomycin (131 μg/ml). All viruses were derived from the HSV-1 KOS strain, the genome of which has been cloned into a bacterial artificial chromosome (BAC), which we received from David Leib (Dartmouth) (Gierasch et al., 2006). For infection assays, Vero cells were grown in DMEM supplemented with 1% FBS, 25 mM HEPES buffer, glutamine (0.3 μg/ml), penicillin, and streptomycin.

Rabbit anti-GFP serum was raised against His_6-GFP, which recognizes both GFP and the His_6tag. UL16 antibodies were raised in rabbits against GST-UL16. Rabbit anti-UL11 serum was raised against GST-UL11. The polyclonal antibody against gE is a generous gift from Harvey M. Friedman (University of Pennsylvania). Rabbit antibodies to VP5 and VP22 were provided by Richard Courtney (Pennsylvania State University College of Medicine). The mouse monoclonal antibody to gD (1D3) was a gift from Gary Cohen and Roselyn Eisenberg (University of Pennsylvania).

4.2. Plasmids

Mammalian expression plasmids for UL16-GFP, UL16(1–155)-GFP and UL16 CTD-GFP have been described elsewhere (Chadha et al., 2012; Yeh et al., 2011). The plasmid for gD.HA was created by adding a HA epitope tag to the C-terminus of gD. All HSV genes in these plasmids are under control of the CMV promoter in the vector pEGFP-N2. The plasmids expressing GST-UL11.1–50, GST-gD.CT, and GST-UL11 were constructed based on the expression vector pGEX-4T-3. The recombinant plasmids pGST-gD.M6 and pGST-gD.M5 were generated by cloning the corresponding gD coding regions (gD.M6: MHRR; gD.M5: MHRRTRKA) in frame with GST sequence into pGEX- 4T-3. The engineering of His_6-UL16 and His_6-UL16 (1–155) into the vector pET-28a has been documented previously (Yeh et al., 2011).

4.3. Purification of GST or His_6-tagged fusion proteins

The detailed protocol for protein purification has been described previously (Yeh et al., 2008). Briefly, bacterial strain BL21 codon plus carrying plasmids for GST or His_6-tagged fusion proteins were cultured at 37 °C in the culture media 2xYT. When OD600 reached 0.6–0.8, protein expression was induced for 3 h by adding IPTG to a final concentration of 0.1 mM. The cells were pelleted at 4 °C, suspended in PBS with protease inhibitor cocktail (P3584, sigma), sonicated, and lysed for 30 min on ice with 1% Triton X-100. The lysate was cleared and the supernatants were incubated with glutathione sepharose 4B beads (GE

Healthcare) or nickel beads at room temperature for 1 h. For GST fusion proteins, the beads were washed 3 times with PBS for 10 min each, and then suspended in PBS. For His-tagged proteins, the beads were washed once with PBS, once with binding buffer, and once with wash buffer. The proteins were eluted with 1 ml elution buffer at room temperature for 3 h.

4.4. GST pull-down assays

To analyze the interaction of UL16 with gD from virus-infected cells, Vero cells were infected with wild-type HSV, UL16 or UL11-null virus at an MOI of 5. To analyze the UL16-gD interaction from transfected cells, Vero cells were transfected with the plasmids carrying UL16-GFP or GFP by Lipofectamine 2000 (Invitrogen) according to the manufacture's protocol. At 18–24 h post infection or transfection, the cells were harvested in NP-40 lysis buffer [0.5% NP-40, 150 mM NaCl, 50 mM Tris-HCl pH 8.0, the protease inhibitor cocktail (P8340, Sigma)], pre-cleared with glutathione-sepharose 4B beads for 2 h at room temperature, and then incubated for 5 h at 37 °C with GST-gE.CT, GST-gD.CT, or GST-UL11 proteins immobilized on glutathione-sepharose beads. The beads were washed three times with NP-40 buffer for 10 min each, boiled for 5 min, and proteins bound to the beads were separated by SDS-PAGE, transferred to nitrocellulose membranes, probed with proper antibodies, and developed by ECL western blotting system (Pierce).

4.5. In vitro binding assay

The *in vitro* binding assay was described previously (Yeh et al., 2008). Briefly, to determine whether UL16 and gD.CT and their derivatives have the ability to interact directly, the purified GST-gD.CT and His_6-UL16 derivatives were incubated in 0.5% NP-40 lysis buffer for 2–3 h at 37 °C. The proteins bound to the beads were washed 3 times with NP-40 buffer, suspended in 30 µl sample buffer, boiled for 5 min, separated by SDS-PAGE, transferred to nitrocellulose, Ponceau S stained, and analyzed by immunoblotting with the anti-His_6 antibody. To determine if the UL16-gD interaction requires cysteines in UL16, purified His_6-UL16(1–155) was pretreated with 10 mM NEM before performing the *in vitro* binding assay.

4.6. Confocal microscopy

Vero cells were grown on coverslips in six-well plates and were transfected with UL16-GFP and gD.HA or its truncation mutants when confluency reached 50–70%. Single transfections of each construct served as control. The cells were fixed with 3.7% paraformaldehyde for 7 min, permeabilized for 10 min with PBS containing 0.1% Triton-100% and 2% BSA, and then blocked with 2% BSA PBS for 30 min gD was stained with mouse monoclonal antibody to HA (Sigma) for 1 h at RT in a humid chamber, and washed 3 times with PBS for 5 min each. After incubation with secondary antibody Alexa-fluor-568-conjugated goat anti-mouse IgG F(ab′)2 fragment (Molecular Probes) for another hour, the cells were washed three times with PBS. Nuclear DNA was stained with DAPI (Molecular Probes). Coverslips were mounted onto slides using Aqua-Poly/mount (Polysciences, Inc.) and images were collected with a Leica SP8 Confocal microscope.

4.7. Construction of mutant viruses

A bacterial artificial chromosome (BAC) containing the HSV-1 KOS strain genome was used to generate mutant viruses using BAC recombineering as previously described (Baird et al., 2010; Gierasch et al., 2006). The UL16 mutant viruses, ΔUL16, ΔUL16.R and ΔUL16.rev35, were constructed during a previous study (Starkey et al., 2014). Briefly, the UL16-null virus was made by deleting the UL16-coding sequence in the genome, and the repaired virus ΔUL16.R was constructed by putting the WT UL16 back to the original U_L16 locus. The mutant ΔUL16.rev35 was constructed in the ΔUL16 BAC by replacing the UL35-coding sequence with UL16-coding sequence. To convert WT HSV-1 KOS into a syncytial strain, a substitution (A855V) was introduced into the cytoplasmic tail of gB to generate HSV.gBsyn (Han et al., 2012). All the gD mutants (Fig. 4) were subsequently made within this parental genome (gBsyn). Specifically, the mutants ΔCT, gD.M5, gD.M6, and gD.M7 were created by adding two stop codons at the corresponding sites (Fig. 4). Other mutants were generated by making small deletions or amino acid substitutions into the gD cytoplasmic tail (Fig. 4). All clones were verified by HindIII digestion and DNA sequencing of the relevant region. Repaired viruses for the mutants ΔCT, M7, AAA, and DED were constructed by replacing the mutated section of the cytoplasmic tail of gD with WT coding sequence. For the M7 and DED mutants constructed without any Syn mutations, the WT HSV-1 KOS BAC was used as the starting point. For the mutants in the gKsyn background, the M7 and DED mutations were built into a BAC containing the gK.A40V Syn mutation.

4.8. Generation of virus stock

BAC plasmids were purified from *E. coli* and transfected into Vero cells using Lipofectamine 2000, as previously described (Baird et al., 2010). At 3–4 days post transfection, when cytopathic effects appeared, transfected cells and media were harvested, and this transfection stock was used to infect new Vero monolayers. Cells and media were harvested 2–3 days post infection, subjected to 3 freeze/thaw rounds, and sonicated to create a working virus stock.

4.9. Packaging assay and viral protein expression

The intracellular expression of viral proteins and their packaging into extracellular virions were measured as previously described (Baird et al., 2010). Briefly, Vero cells were infected with the indicated viruses at an MOI of 5. At 18–24 h post infection, extracellular virions were harvested from the media via centrifugation through a 30% sucrose cushion for 1 h at 83,500 × *g* in a Beckman SW41 rotor at 4 °C. The pelleted virions were then resuspended in sample buffer. Cell lysates were harvested by pelleting infected cells, resuspending them in sample buffer, and sonicating the samples. Both the virions and the cell lysate samples were resolved on SDS-PAGE gels prior to analysis by western blotting with antibodies against the specified viral proteins.

4.10. Viral replication assays

6-well plates of Vero cells were infected with the specified viruses at a multiplicity of infection (MOI) of 0.1 or 5. After 1 h incubation at 37 °C, the cells were first washed with acid buffer (135 mM NaCl, 10 mM KCl, 40 mM citric acid, PH 3.0), then once with DMEM, and overlaid with 1 ml DMEM containing 2% FBS. At indicated times post-infection, cells were scraped off the plates. Media was separated from cells by centrifugation at 12,000 rpm for 1 min, and frozen at −80 °C. Cells were washed three times with DMEM, and freeze-thawed 3 times to release cell-associated viruses. Each sample was titrated on Vero cells using a standard viral plaque assay.

4.11. Imaging the Syn phenotype

For the gD mutants in the gBsyn background, Vero cells were infected with the specified viruses at a multiplicity of infection (MOI) of 0.001. After 1 h incubation at 37 °C, the inoculum was removed and the cells were first washed DMEM before being overlaid with DMEM containing 1% FBS and 0.5% agarose. At 48 h post infection, the cells were examined for syncytium formation under an inverted light microscope (Olympus). For M7 and DED in the gKsyn background, Vero cells were infected at low MOI (0.001) for 1 h at 37 °C, after which the inoculum was removed, cells were rinsed one time with DMEM, and the cells were

incubated with DMEM containing 2% FBS. Individual syncytia were imaged at 24 or 48 h post infection.

4.12. Cell-to-cell spread assay

Vero cells seeded on coverslips were infected with WT, M7, or DED viruses at a low MOI (0.001) for 1 h at 37 °C. After infection, cells were rinsed once with DMEM and overlaid with DMEM containing 2% FBS and 5 mg/ml pooled human IgG (Equitech Bio). This amount of pooled IgG was previously determined to contain enough neutralizing antibodies to neutralize all cell-free virus (Carmichael et al., 2018). At 48 h post infection, cells were fixed with 3.7% PFA for 10 min, permeabilized with PBS containing 0.1% Triton-100% and 2% BSA, and then blocked with 2% BSA PBS for 30 min. The cells were then stained with rabbit antibodies to VP5 (1:1000) for 1 h, rinsed 3 times, and stained with the secondary antibody Alexa 568 secondary antibody (1:1000) for 1 h. Finally, cells were stained with DAPI for 5 min and the coverslips were mounted onto slides. Fluorescent images of VP5-positive cells were captured with an Olympus IX73 inverted microscopes and plaque area was determined using the Olympus cellSens software.

4.13. Flow cytometry fusion assay

This protocol has been described elsewhere (Carmichael et al., 2018). Briefly, confluent Vero cells in 6-well plates were infected with WT KOS, M7, or DED viruses at an MOI of 3 for 1 h at 37 °C. After infection, cells were incubated in DMEM with 2% FBS containing DMSO (vehicle) or 50 μM salubrinal (Sigma-Aldrich). At 18 h post infection, cells were rinsed once with standard buffer and 400 μl trypsin was added to each well. Once cells lifted off the plate, 600 μl of ice-cold 4% PFA/PBS (EMS) was added to the well and pipetted up and down vigorously to break open any syncytia. The samples were then allocated to flow cytometry tubes on ice and the wells were rinsed with 200 μl of FACS buffer (2% BSA, 3 mM EDTA in Ca^{2+}/Mg^{2+}-free PBS), which was added to the respective tubes. Samples were stained with 200 μl propidium iodide solution (100 μg/ml in FACS buffer; ThermoFisher), vortexed, and analyzed by BD LSRFortessa cell analyzer. 50,000 events were gathered per sample and data analysis was done using FlowJo software. PI-positive events were gated for FSA (forward scatter) and SSC (side scatter) to determine their size and granularity, effectively distinguishing between populations of intact single cells and nuclei that had been freed from syncytia. The percentage of free nuclei per sample was used to estimate total fusion.

4.14. Statistical analysis

The statistical analyses were performed by using Student *T* test with two tailed distribution using GraphPad Prism (version 4). The significance values were represented as follows: *: $P < 0.05$, **: $P < 0.01$, ***: $P < 0.001$, and ****: $P < 0.0001$. NS: no statistical significance.

Acknowledgements

We would like to thank Carol Wilson for providing technical support for these experiments. We would also like to acknowledge Nicholas Buchkovich (Penn State College of Medicine) for assistance with editing the manuscript.

Funding information

This study was supported by the Chinese Thousand Youth Talents award (1051-21986001) and a K99 Award (1K99AI110648-01) to J.H. and NIH grant (AI071286) to J.W.W, which provided support for A.S., J.C.C., and P.C. In addition, J.L.S. and D.Z. were supported in part by NIH training grant T32CA060395.

References

Ambrosini, A., Enquist, L., 2015. Cell-fusion events induced by alpha-herpesviruses. Future medicine. Future Virol. 185–200.
Arii, J., Shindo, K., Koyanagi, N., Kato, A., Kawaguchi, Y., 2016. Multiple roles of the cytoplasmic domain of herpes simplex virus 1 envelope glycoprotein D in infected cells. J. Virol. 90, 10170–10181.
Atanasiu, D., Saw, W.T., Cohen, G.H., Eisenberg, R.J., 2010. Cascade of events governing cell-cell fusion induced by herpes simplex virus glycoproteins gD, gH/gL, and gB. J. Virol. 84, 12292–12299.
Baird, N.L., Starkey, J.L., Hughes, D.J., Wills, J.W., 2010. Myristylation and palmitylation of HSV-1 UL11 are not essential for its function. Virology 397, 80–88.
Balan, P., Davis-Poynter, N., Bell, S., Atkinson, H., Browne, H., Minson, T., 1994. An analysis of the in vitro and in vivo phenotypes of mutants of herpes simplex virus type 1 lacking glycoproteins gG, gE, gI or the putative gJ. J. Gen. Virol. 75 (Pt 6), 1245–1258.
Bond, V.C., Person, S., 1984. Fine structure physical map locations of alterations that affect cell fusion in herpes simplex virus type 1. Virology 132, 368–376.
Boyce, M., Bryant, K.F., Jousse, C., Long, K., Harding, H.P., Scheuner, D., Kaufman, R.J., Ma, D., Coen, D.M., Ron, D., Yuan, J., 2005. A selective inhibitor of eIF2alpha dephosphorylation protects cells from ER stress. Science 307, 935–939.
Browne, H., Bruun, B., Whiteley, A., Minson, T., 2003. Analysis of the role of the membrane-spanning and cytoplasmic tail domains of herpes simplex virus type 1 glycoprotein D in membrane fusion. J. Gen. Virol. 84, 1085–1089.
Bryant, K.F., Macari, E.R., Malik, N., Boyce, M., Yuan, J., Coen, D.M., 2008. ICP34.5-dependent and -independent activities of salubrinal in herpes simplex virus-1 infected cells. Virology 379, 197–204.
Carmichael, J.C., Yokota, H., Craven, R.C., Schmitt, A., Wills, J.W., 2018. The HSV-1 mechanisms of cell-to-cell spread and fusion are critically dependent on host PTP1B. PLoS Pathog. 14, e1007054.
Ch'ng, T.H., Spear, P.G., Struyf, F., Enquist, L.W., 2007. Glycoprotein D-independent spread of pseudorabies virus infection in cultured peripheral nervous system neurons in a compartmented system. J. Virol. 81, 10742–10757.
Chadha, P., Han, J., Starkey, J.L., Wills, J.W., 2012. Regulated interaction of tegument proteins UL16 and UL11 from herpes simplex virus. J. Virol. 86, 11886–11898.
Chatterjee, S., Koga, J., Whitley, R.J., 1989. A role for herpes simplex virus type 1 glycoprotein E in induction of cell fusion. J. Gen. Virol. 70 (Pt 8), 2157–2162.
Cheshenko, N., Herold, B.C., 2002. Glycoprotein B plays a predominant role in mediating herpes simplex virus type 2 attachment and is required for entry and cell-to-cell spread. J. Gen. Virol. 83, 2247–2255.
Chi, J.H., Harley, C.A., Mukhopadhyay, A., Wilson, D.W., 2005. The cytoplasmic tail of herpes simplex virus envelope glycoprotein D binds to the tegument protein VP22 and to capsids. J. Gen. Virol. 86, 253–261.
Cocchi, F., Fusco, D., Menotti, L., Gianni, T., Eisenberg, R.J., Cohen, G.H., Campadelli-Fiume, G., 2004. The soluble ectodomain of herpes simplex virus gD contains a membrane-proximal pro-fusion domain and suffices to mediate virus entry. Proc. Natl. Acad. Sci. USA 101, 7445–7450.
Cooper, R.S., Heldwein, E.E., 2015. Herpesvirus gB: a finely tuned fusion machine. Viruses 7, 6552–6569.
Davis-Poynter, N., Bell, S., Minson, T., Browne, H., 1994. Analysis of the contributions of herpes simplex virus type 1 membrane proteins to the induction of cell-cell fusion. J. Virol. 68, 7586–7590.
Debroy, C., Pederson, N., Person, S., 1985. Nucleotide sequence of a herpes simplex virus type 1 gene that causes cell fusion. Virology 145, 36–48.
Desai, P., DeLuca, N.A., Person, S., 1998. Herpes simplex virus type 1 VP26 is not essential for replication in cell culture but influences production of infectious virus in the nervous system of infected mice. Virology 247, 115–124.
Dingwell, K.S., Brunetti, C.R., Hendricks, R.L., Tang, Q., Tang, M., Rainbow, A.J., Johnson, D.C., 1994. Herpes simplex virus glycoproteins E and I facilitate cell-to-cell spread in vivo and across junctions of cultured cells. J. Virol. 68, 834–845.
Dingwell, K.S., Doering, L.C., Johnson, D.C., 1995. Glycoproteins E and I facilitate neuron-to-neuron spread of herpes simplex virus. J. Virol. 69, 7087–7098.
Dolter, K.E., Ramaswamy, R., Holland, T.C., 1994. Syncytial mutations in the herpes simplex virus type 1 gK (UL53) gene occur in two distinct domains. J. Virol. 68, 8277–8281.
El Kasmi, I., Lippé, R., 2015. Herpes simplex virus 1 gN partners with gM to modulate the viral fusion machinery. J. Virol. 89, 2313–2323.
Fantini, J., Di Scala, C., Baier, C.J., Barrantes, F.J., 2016. Molecular mechanisms of protein-cholesterol interactions in plasma membranes: functional distinction between topological (tilted) and consensus (CARC/CRAC) domains. Chem. Phys. Lipids 199, 52–60.
Farnsworth, A., Goldsmith, K., Johnson, D.C., 2003. Herpes simplex virus glycoproteins gD and gE/gI serve essential but redundant functions during acquisition of the virion envelope in the cytoplasm. J. Virol. 77, 8481–8494.
Feenstra, V., Hodaie, M., Johnson, D.C., 1990. Deletions in herpes simplex virus glycoprotein D define nonessential and essential domains. J. Virol. 64, 2096–2102.
Fulmer, P.A., Melancon, J.M., Baines, J.D., Kousoulas, K.G., 2007. UL20 protein functions precede and are required for the UL11 functions of herpes simplex virus type 1 cytoplasmic virion envelopment. J. Virol. 81, 3097–3108.
Fusco, D., Forghieri, C., Campadelli-Fiume, G., 2005. The pro-fusion domain of herpes simplex virus glycoprotein D (gD) interacts with the gD N terminus and is displaced by soluble forms of viral receptors. Proc. Natl. Acad. Sci. USA 102, 9323–9328.
Gage, P.J., Levine, M., Glorioso, J.C., 1993. Syncytium-inducing mutations localize to two discrete regions within the cytoplasmic domain of herpes simplex virus type 1 glycoprotein B. J. Virol. 67, 2191–2201.

Geraghty, R.J., Krummenacher, C., Cohen, G.H., Eisenberg, R.J., Spear, P.G., 1998. Entry of alphaherpesviruses mediated by poliovirus receptor-related protein 1 and poliovirus receptor. Science 280, 1618–1620.
Gierasch, W.W., Zimmerman, D.L., Ward, S.L., Vanheyningen, T.K., Romine, J.D., Leib, D.A., 2006. Construction and characterization of bacterial artificial chromosomes containing HSV-1 strains 17 and KOS. J. Virol. Methods 135, 197–206.
Gross, S.T., Harley, C.A., Wilson, D.W., 2003. The cytoplasmic tail of Herpes simplex virus glycoprotein H binds to the tegument protein VP16 in vitro and in vivo. Virology 317, 1–12.
Haanes, E.J., Nelson, C.M., Soule, C.L., Goodman, J.L., 1994. The UL45 gene product is required for herpes simplex virus type 1 glycoprotein B-induced fusion. J. Virol. 68, 5825–5834.
Han, J., Chadha, P., Meckes, D.G., Baird Jr., N.L., Wills, J.W., 2011. Interaction and interdependent packaging of tegument protein UL11 and glycoprotein e of herpes simplex virus. J. Virol. 85, 9437–9446.
Han, J., Chadha, P., Starkey, J.L., Wills, J.W., 2012. Function of glycoprotein E of herpes simplex virus requires coordinated assembly of three tegument proteins on its cytoplasmic tail. Proc. Natl. Acad. Sci. USA 109, 19798–19803.
Hanssens, F.P., Nauwynck, H.J., Mettenlieter, T.C., 1995. Role of glycoprotein gD in the adhesion of pseudorabies virus infected cells and subsequent cell-associated virus spread. Arch. Virol. 140, 1855–1862.
Heldwein, E.E., Krummenacher, C., 2008. Entry of herpesviruses into mammalian cells. Cell. Mol. Life Sci.: CMLS 65, 1653–1668.
Hutchinson, L., Goldsmith, K., Snoddy, D., Ghosh, H., Graham, F.L., Johnson, D.C., 1992. Identification and characterization of a novel herpes simplex virus glycoprotein, gK, involved in cell fusion. J. Virol. 66, 5603–5609.
Johnson, D.C., Huber, M.T., 2002. Directed egress of animal viruses promotes cell-to-cell spread. J. Virol. 76, 1–8.
Johnson, D.C., Ligas, M.W., 1988. Herpes simplex viruses lacking glycoprotein D are unable to inhibit virus penetration: quantitative evidence for virus-specific cell surface receptors. J. Virol. 62, 4605–4612.
Johnson, D.C., Wisner, T.W., Wright, C.C., 2011. Herpes simplex virus glycoproteins gB and gD function in a redundant fashion to promote secondary envelopment. J. Virol. 85, 4910–4926.
Kim, I.J., Chouljenko, V.N., Walker, J.D., Kousoulas, K.G., 2013. Herpes simplex virus 1 glycoprotein M and the membrane-associated protein UL11 are required for virus-induced cell fusion and efficient virus entry. J. Virol. 87, 8029–8037.
Kramer, T., Enquist, L.W., 2013. Directional spread of alphaherpesviruses in the nervous system. Viruses 5, 678–707.
Krummenacher, C., Nicola, A.V., Whitbeck, J.C., Lou, H., Hou, W., Lambris, J.D., Geraghty, R.J., Spear, P.G., Cohen, G.H., Eisenberg, R.J., 1998. Herpes simplex virus glycoprotein D can bind to poliovirus receptor-related protein 1 or herpesvirus entry mediator, two structurally unrelated mediators of virus entry. J. Virol. 72, 7064–7074.
Lee, H.C., Chouljenko, V.N., Chouljenko, D.V., Boudreaux, M.J., Kousoulas, K.G., 2009. The herpes simplex virus type 1 glycoprotein D (gD) cytoplasmic terminus and full-length gE are not essential and do not function in a redundant manner for cytoplasmic virion envelopment and egress. J. Virol. 83, 6115–6124.
Leege, T., Fuchs, W., Granzow, H., Kopp, M., Klupp, B.G., Mettenleiter, T.C., 2009. Effects of simultaneous deletion of pUL11 and glycoprotein M on virion maturation of herpes simplex virus type 1. J. Virol. 83, 896–907.
Ligas, M.W., Johnson, D.C., 1988. A herpes simplex virus mutant in which glycoprotein D sequences are replaced by beta-galactosidase sequences binds to but is unable to penetrate into cells. J. Virol. 62, 1486–1494.
Looker, K.J., Magaret, A.S., May, M.T., Turner, K.M., Vickerman, P., Gottlieb, S.L., Newman, L.M., 2015. Global and regional estimates of prevalent and incident herpes simplex virus type 1 infections in 2012. PLoS One 10, e0140765.
Loomis, J.S., Courtney, R.J., Wills, J.W., 2003. Binding partners for the UL11 tegument protein of herpes simplex virus type 1. J. Virol. 77, 11417–11424.
Mateo, M., Generous, A., Sinn, P.L., Cattaneo, R., 2015. Connections matter–how viruses use cell–cell adhesion components. J. Cell Sci. 128, 431–439.
McGraw, H.M., Friedman, H.M., 2009. Herpes simplex virus type 1 glycoprotein E mediates retrograde spread from epithelial cells to neurites. J. Virol. 83, 4791–4799.
Meckes, D.G., Wills Jr., J.W., 2007. Dynamic interactions of the UL16 tegument protein with the capsid of herpes simplex virus. J. Virol. 81, 13028–13036.
Meckes, D.G., Wills Jr., J.W., 2008. Structural rearrangement within an enveloped virus upon binding to the host cell. J. Virol. 82, 10429–10435.
Meckes, D.G., Marsh, J.A., Wills, J.W., 2010. Complex mechanisms for the packaging of the UL16 tegument protein into herpes simplex virus. Virology 398, 208–213.
Melancon, J.M., Foster, T.P., Kousoulas, K.G., 2004. Genetic analysis of the herpes simplex virus type 1 UL20 protein domains involved in cytoplasmic virion envelopment and virus-induced cell fusion. J. Virol. 78, 7329–7343.
Neidhardt, H., Schröder, C.H., Kaerner, H.C., 1987. Herpes simplex virus type 1 glycoprotein E is not indispensable for viral infectivity. J. Virol. 61, 600–603.
O'Regan, K.J., Brignati, M.J., Murphy, M.A., Bucks, M.A., Courtney, R.J., 2010. Virion incorporation of the herpes simplex virus type 1 tegument protein VP22 is facilitated by trans-Golgi network localization and is independent of interaction with glycoprotein E. Virology 405, 176–192.
Pogue-Geile, K.L., Lee, G.T., Shapira, S.K., Spear, P.G., 1984. Fine mapping of mutations in the fusion-inducing MP strain of herpes simplex virus type 1. Virology 136, 100–109.
Polcicova, K., Goldsmith, K., Rainish, B.L., Wisner, T.W., Johnson, D.C., 2005. The extracellular domain of herpes simplex virus gE is indispensable for efficient cell-to-cell spread: evidence for gE/gI receptors. J. Virol. 79, 11990–12001.
Saldanha, C.E., Lubinski, J., Martin, C., Nagashunmugam, T., Wang, L., van Der Keyl, H., Tal-Singer, R., Friedman, H.M., 2000. Herpes simplex virus type 1 glycoprotein E domains involved in virus spread and disease. J. Virol. 74, 6712–6719.
Sanders, P.G., Wilkie, N.M., Davison, A.J., 1982. Thymidine kinase deletion mutants of herpes simplex virus type 1. J. Gen. Virol. 63, 277–295.
Sarfo, A., Starkey, J., Mellinger, E., Zhang, D., Chadha, P., Carmichael, J., Wills, J.W., 2017. The UL21 tegument protein of herpes simplex virus 1 is differentially required for the syncytial phenotype. J. Virol. 91.
Sattentau, Q., 2008. Avoiding the void: cell-to-cell spread of human viruses. Nat. Rev. Microbiol. 6, 815–826.
Shukla, D., Liu, J., Blaiklock, P., Shworak, N.W., Bai, X., Esko, J.D., Cohen, G.H., Eisenberg, R.J., Rosenberg, R.D., Spear, P.G., 1999. A novel role for 3-O-sulfated heparan sulfate in herpes simplex virus 1 entry. Cell 99, 13–22.
Smith, G., 2012. Herpesvirus transport to the nervous system and back again. Annu. Rev. Microbiol. 66, 153–176.
Spear, P.G., Manoj, S., Yoon, M., Jogger, C.R., Zago, A., Myscofski, D., 2006. Different receptors binding to distinct interfaces on herpes simplex virus gD can trigger events leading to cell fusion and viral entry. Virology 344, 17–24.
Starkey, J.L., Han, J., Chadha, P., Marsh, J.A., Wills, J.W., 2014. Elucidation of the block to herpes simplex virus egress in the absence of tegument protein UL16 reveals a novel interaction with VP22. J. Virol. 88, 110–119.
Subramanian, R.P., Geraghty, R.J., 2007. Herpes simplex virus type 1 mediates fusion through a hemifusion intermediate by sequential activity of glycoproteins D, H, L, and B. Proc. Natl. Acad. Sci. USA 104, 2903–2908.
Tsvitov, M., Frampton, A.R., Shah Jr., W.A., Wendell, S.K., Ozuer, A., Kapacee, Z., Goins, W.F., Cohen, J.B., Glorioso, J.C., 2007. Characterization of soluble glycoprotein D-mediated herpes simplex virus type 1 infection. Virology 360, 477–491.
Turner, A., Bruun, B., Minson, T., Browne, H., 1998. Glycoproteins gB, gD, and gHgL of herpes simplex virus type 1 are necessary and sufficient to mediate membrane fusion in a Cos cell transfection system. J. Virol. 72, 873–875.
Wheeler, C., 1960. Herpes simplex virus. Characteristics of a strain which produces unusually large multinucleated giat cells in tissue culture. Arch. Dermatol. 82, 391–399.
Whitbeck, J.C., Peng, C., Lou, H., Xu, R., Willis, S.H., Ponce de Leon, M., Peng, T., Nicola, A.V., Montgomery, R.I., Warner, M.S., Soulika, A.M., Spruce, L.A., Moore, W.T., Lambris, J.D., Spear, P.G., Cohen, G.H., Eisenberg, R.J., 1997. Glycoprotein D of herpes simplex virus (HSV) binds directly to HVEM, a member of the tumor necrosis factor receptor superfamily and a mediator of HSV entry. J. Virol. 71, 6083–6093.
Wisner, T.W., Johnson, D.C., 2004. Redistribution of cellular and herpes simplex virus proteins from the trans-golgi network to cell junctions without enveloped capsids. J. Virol. 78, 11519–11535.
Yeh, P.C., Han, J., Chadha, P., Meckes, D.G., Ward Jr., M.D., Semmes, O.J., Wills, J.W., 2011. Direct and specific binding of the UL16 tegument protein of herpes simplex virus to the cytoplasmic tail of glycoprotein E. J. Virol. 85, 9425–9436.
Yeh, P.C., Meckes, D.G., Wills Jr., J.W., 2008. Analysis of the interaction between the UL11 and UL16 tegument proteins of herpes simplex virus. J. Virol. 82, 10693–10700.
Zago, A., Jogger, C.R., Spear, P.G., 2004. Use of herpes simplex virus and pseudorabies virus chimeric glycoprotein D molecules to identify regions critical for membrane fusion. Proc. Natl. Acad. Sci. USA 101, 17498–17503.